Dynamic regulation of key players of embryo implantation and fertility in human uterine extracellular vesicles during menstrual cycle

Alin Rai[1], Qi Hui Poh[1,2], Monique Fatmous[1,2], Haoyun Fang[1], Shanti Gurung[3], Beverley Vollenhoven[4,5,6], Lois A Salamonsen[3,7], David W Greening[1,2*]

[1]Baker Heart and Diabetes Institute, Molecular Proteomics, Melbourne, Victoria, 3004, Australia. [2]Department of Biochemistry and Genetics, La Trobe Institute for Molecular Science, La Trobe University, Bundoora, Victoria, 3086, Australia. [3]Hudson Institute of Medical Research, Clayton, Victoria, 3168, Australia. [4]Department of Obstetrics and Gynaecology, Monash University, Clayton, Victoria, 3168, Australia, [5]Monash IVF, Clayton, Victoria, 3168, Australia. [6] Women's and Newborn Program, Monash Health. [7]Department of Molecular and Translational Science, Monash University, Clayton, Victoria, 3168, Australia.

*To whom correspondence should be addressed:

Dr David W. Greening

Molecular Proteomics, Baker Heart and Diabetes Institute

75 Commercial Road, Melbourne, 3004, Australia

Email: David.Greening@baker.edu.au

Abstract

Endometrial extracellular vesicles (EVs) are emerging as important players in reproductive biology. However, how their proteome is regulated throughout the menstrual cycle is not known. Such information can provide novel insights into biological processes critical for embryo development, implantation and successful pregnancy. Using mass spectrometry-based quantitative proteomics, we show that small EVs (sEVs) isolated from uterine lavage of fertile women (UL-sEV), compared to infertile women, are laden with proteins implicated in antioxidant activity (SOD1, GSTO1, MPO, CAT). Functionally, sEVs derived from endometrial cells enhance antioxidant function (tert-butyl hydrogen peroxide scavenging activity) in trophectoderm cells. Moreover, there was striking enrichment of invasion-related proteins (LGALS1/3, S100A4/11) in fertile UL-sEVs in the secretory (estrogen plus progesterone-driven, EP) *versus* proliferative (estrogen-driven, E) phase, with several players downregulated in infertile UL-sEVs. Consistent with this, sEVs from EP- *versus* E-primed endometrial epithelial cells (Ishikawa) promote invasion of trophectoderm cells into Matrigel^{TM}. Compared to UL-sEVs, the soluble secretome in uterine lavages from fertile women was enriched in proteins involved in glycolysis and chaperones that ensure telomere maintenance. Interestingly, UL-sEVs from fertile versus infertile women carry known players/predictors of embryo implantation (PRDX2, IDHC), endometrial receptivity (S100A4, FGB, SERPING1, CLU, ANXA2) and implantation success (CAT, YWHAE, PPIA), highlighting their potential to inform regarding endometrial status/pregnancy outcomes. Thus, this study provides novel insights into proteome reprogramming of sEVs and the soluble secretome in uterine fluid, with potential to enhance embryo implantation and hence fertility.

Keywords

extracellular vesicles, uterine fluid, embryo implantation, fertility, proteomics

Introduction

Uterine fluid provides a conducive environment for pre-implantation embryo survival/ growth and mediates embryo-maternal crosstalk critical for implantation and pregnancy establishment [1-3]. The molecular composition of uterine fluid, encompasses protein-rich histotroph secretions from glandular epithelium and proteins selectively transudated from systemic circulation, along with ions, amino acids, lipids and other mediators, and this is tightly regulated by maternal hormones estrogen (as estradiol 17β, E) and progesterone (P), and embryonic signals [4]. In women, transition of endometrium from proliferative (P-phase) towards secretory (S-phase) phase involves maturation of secretory glands and reprogramming of the uterine fluid composition through secretion of factors that regulate embryo development and implantation [5]. Direct interference with this composition (for example, by ablating endometrial glands or their secretory capacity) compromises embryo development/survival [6] and blastocyst implantation [7]. Uterine fluid also exerts long lasting epigenetic imprints on the pre-implantation embryo, hence impacting fetal development and health of the baby [5]. Comprehensive identification of proteins and secretory factors in human uterine fluid has been performed in different phases of the menstrual cycle (including secretory [8] and mid-secretory phases [9]), differing endometrial receptivity stages [9,10] and embryo implantation outcomes [11,12]. Such systemic profiling of uterine fluid has provided valuable insights into biological processes regulating pregnancy establishment, and now holds promise as an endometrial tissue biopsy-surrogate to monitor the window of implantation (WoI), identify the underlying etiology of recurrent implantation failure [13], predict implantation success in IVF cycles [12], guide timings of embryo transfer and enable design of non-hormonal based contraceptives.

It is now evident that crucial components of uterine fluid, distinct from the soluble secretome (SS), are nano-sized membrane-bound structures released by cells, called extracellular vesicles (EVs) [14,15]. Several studies have catalogued their role in mediating fetal-maternal crosstalk [14,16,17]. EVs do this by selectively packaging proteins and nucleic acids, which they can transfer between cells (protected from extracellular degradation) to elicit a functional response [18]. The functional spectrum of EVs in reproductive biology is now expanding [16], and includes sperm motility and activation [19], capacitation

[20], acrosome reaction [21,22], oocyte maturation [23], fertilization [24], and embryo-maternal crosstalk [25]. We were the first to report that EVs are found in human uterine fluid and are readily isolated using differential centrifugation [14,15]. Moreover, protein composition of a major class of EVs called small EVs (sEVs, also referred to as exosomes) released by endometrial cells are actively regulated by ovarian hormones E and P [26]. We recently demonstrated that these sEVs significantly increased total cell number in mouse embryos, hatching from zona pellucida, and enhanced embryo outgrowth and implantation rate [27].

While we have demonstrated that human endometrial epithelial sEV protein composition is regulated by the hormones estrogen and progesterone *in vitro* [26], whether this is reflected *in vivo* in the EVs released into uterine fluid during the menstrual cycle remains unknown. Importantly, whether these sEVs differ in their protein content between fertile and infertile women warrants investigation. However, identifying proteome composition of sEVs within human uterine fluid on a whole-proteome scale has remained a technical challenge, mainly due to the very low volumes of uterine fluid (≤50 µL) and hence the low numbers of sEVs that can be isolated from it: we can obtain only ~1-2 µg sEVs from uterine fluid from any individual, far too low for traditional western-blot-based analyses. In this study, we performed high-resolution quantitative mass spectrometry-based proteomic profiling of the sEVs from uterine fluid of individual women with proven fertility during the proliferative and secretory phases of the menstrual cycle and compared these with profiles of similar sEVs from infertile women. Our data reveal a dynamic regulation of key players of embryo implantation and fertility during the menstrual cycle of human uterine fluid sEVs and uncover, for the first time, regulators of key biological processes enriched in uterine fluid sEVs between fertile *versus* infertile women.

Results

Isolation of sEVs from uterine lavage

The patient cohort for preparation of soluble secretome (SS) and sEVs from uterine lavage (UL) is shown in **Table 1**, along with the protein yields of SS and sEVs. **Fig. 1a** details the sequential centrifugation procedure utilized. The terminology used henceforth for the preparations is UL-T for total protein, UL-SS and UL-sEVs. Cryo-electron microscopy revealed that UL-sEVs displayed spherical morphology and were ~50-80 nm in diameter **(Fig. 1b-c)**, consistent with previous reports [28,29]. There were no differences in size between proliferative phase (P-phase) and secretory phase (S-phase) or between fertile and infertile women.

UL-sEVs are internalized by human trophectoderm cells

To assess whether sEVs isolated from the UL can be taken up by human trophectoderm, we labelled UL-sEVs using lipophilic tracer DiI and incubated them with trophectoderm cells [17] for 2 h. Confocal microscopy revealed that UL-sEVs from both fertile and infertile women are readily taken up by trophectoderm cells **(Fig. 2)**.

Proteomic analysis reveals differences between protein content of UL-sEVs, UL-T and UL-SS

To gain insight into the function of UL-sEVs, we analyzed their protein composition using quantitative mass spectrometry. We also concurrently performed proteome profiling of UL-T and UL-SS for comparative analysis. A total of 682, 460 and 240 proteins were identified in UL-T, UL-SS and UL-sEVs, respectively (**Fig. 3a, Supplementary Tables S1-S3**), which, to our knowledge, is the most comprehensive uterine lavage proteome to date (unstimulated menstrual cycle). Gene Ontology (GO) analysis revealed that 197/240 UL-sEV proteins have been previously found in sEVs including exosomes with 201/240 (84%) proteins reported in the exosome database ExoCarta [30]. We noted that compared to P-phase, S-phase UL-T displayed greater proteome complexity **(Supplementary Fig. S2)**: this is likely due to altered protein synthesis as the endometrium transitions towards a secretory phenotype. Principal component analysis (PCA) of identified proteins and their reporter ion intensities

(abundance) revealed that UL-T, UL-SS and UL-sEVs are all molecularly distinct between the P- and S-phases **(Fig. 3b)**.

UL-sEVs are enriched in proteins that regulate antioxidant activity

A total of 200 and 206 proteins were identified in P- and S-phase UL-sEVs, respectively **(Supplementary Table S3)**. To gain insight into the function of UL-sEVs, we created an EnrichmentMap of biological processes and pathways overrepresented in the proteome of P-phase UL-sEVs **(Fig. 3c, Supplementary Table S4)** and S-phase UL-sEVs **(Fig. 3d, Supplementary Table S5)**. P-phase UL-sEVs were enriched in proteins implicated in immune regulation, lipid metabolism, antioxidant activity, antimicrobial function, mucosal immunity, glycolysis and coagulation/fibrinolysis **(Fig. 3c)**. In addition to these processes, S-phase UL-sEVs were enriched in proteins implicated in mitochondrial regulation and ion homeostasis **(Fig. 3d)**.

Between P-phase and S-phase UL-sEVs, striking enrichment of antioxidant proteins (e.g., MPO, PRDX1/2, TXN, PARK7) includes those that are implicated in "cellular antioxidant detoxification", "response to reactive oxygen species (ROS)", "hydrogen peroxide catabolic process", "removal of super oxide radicals" and "hydrogen peroxide metabolic process" amongst others **(Fig. 3c-d)**. Antioxidants ensure a delicate balance of ROS generated under normal physiological conditions, with excessive ROS causing embryo defects, implantation failure and pregnancy loss [31,32].

Our data suggests that UL-sEVs potentially display antioxidant activity. This hypothesis was tested. Given the unavailability of sufficient UL-sEVs for functional studies, we purified sEVs released by human endometrial epithelial cells (Ishikawa cells) that were hormonally primed with estrogen (E-sEVs) and subsequently with E and progesterone (EP-sEVs) to recapitulate P-phase and S-phase, respectively, as previously described [26]. These were applied to trophectoderm cells along with the ROS activator tert-butyl hydrogen peroxide (TBHP), and ROS activity assessed. Similar to the antioxidant L-ascorbic acid (used as a positive control [33], both E- and EP-sEVs significantly reduced TBHP-induced ROS activity in trophectoderm cells **(Fig. 3e)**. Moreover, proteomic dissection of UL-sEVs from fertile

(200 proteins) and infertile (187 proteins) women (**Fig. 3f, Supplementary Table S6**) revealed that proteins downregulated during infertility (79 proteins) include those that are implicated in antioxidant function (e.g., APOE, BLVRB, CAT, GSTO1, HBA2/G1, MPO, S100A9, SOD1) (**Fig. 3g, Supplementary Table S7**). Several of these antioxidants, including SOD1, APOE and GSTO1, were also present in human endometrial epithelial cell-derived sEVs [26] (**Fig. 3c,d,g**). Thus, our findings highlight the role of UL-sEVs in potentially protecting the embryo against ROS-mediated damages within the uterine microenvironment.

UL-sEVs are enriched in invasion-related proteins

We next questioned whether P- and S-phase UL-sEVs carry out distinct functions. Compared to P-phase UL-sEVs, a total of 64 proteins (34 uniquely identified and 30 upregulated, fold change >1.5) were found in higher abundance in S-phase sEVs **(Fig. 4a, Supplementary Table S3)**. Strikingly, 32/64 of these proteins were implicated in cell invasion **(Table 2)**. Pre-eminent among these are LGALS1 [34], LGALS3 [35] and VIM [36] which can directly promote trophoblast invasion [34-36]. Thus, our data suggests that S-phase UL-sEVs will promote invasive capacity in trophectoderm cells, a phenotype essential for successful embryo implantation [37]. To test this hypothesis, we prepared spheroids from trophectoderm cells (blastocyst mimics), exposed these to endometrial epithelial sEVs (E and EP-treated) and assessed their capacity to invade into Matrigel™ [17]. Endometrial epithelial sEVs were readily taken up by trophectoderm spheroids within 2 h **(Supplementary Fig. S3)**. Compared to control spheroids or those treated with E-sEVs, spheroids treated with EP-sEVs displayed significant levels of invasive outgrowth **(Fig. 4b)**. Importantly, several of these invasion-related proteins in S-phase UL-sEVs (namely, AHNAK, APOC1, CA2, MPO, S100A1, SERPINA3, SPRR3) were significantly downregulated in UL-sEVs from infertile women **(Fig. 4c)**. Furthermore, additional invasion-related proteins were down regulated in UL-sEVs during infertility **(Table 3)**. Several of these proteins, including SOD1, PRDX6, PRDX1, TMP4 and PARK7, were also upregulated in human endometrial epithelial cell-derived EP-*versus* E-sEVs [26] (**Fig. 4a**). Thus, our data indicates that phase-specific reprogramming of UL-sEVs potentially enhances trophectoderm invasion to support embryo implantation.

Phase-specific reprogramming of UL total protein and UL-sEVs in fertile women

To obtain a comprehensive insight into biological pathways and processes enriched within the uterine environment, we next assessed phase-specific reprogramming of UL-T **(Supplementary Table S8)** and UL-sEVs **(Supplementary Table S9)** proteomic landscape in fertile women. Consistent with P- to S-phase transition of the endometrium [38], S-phase UL-T proteins were enriched in biological processes involved in cell cycle regulation and morphogenesis **(Fig. 5)**. Critical pathways enriched in S-phase UL-T include chaperone-mediated protein folding (via heat shock proteins) and telomere maintenance (via chaperonin containing TCP1 complex components) which are essential for embryo health, protection and implantation to the endometrium [39-41]. A striking finding during P- to S-phase transition in UL-T was marked enrichment of proteins involved in glycolysis and pentose phosphate pathway, consistent with the metabolic needs of pre-implantation human blastocyst [42]. Importantly, similar to UL-sEVs, UL-T was also enriched in proteins implicated in antioxidant activity involving hydrogen peroxide catabolic process, and glutathione metabolism and conjugation **(Fig. 5)**, suggesting that UL-T and UL-sEVs collectively protect the pre-implantation embryo from ROS-mediated damage.

Differential protein expression in UL-proliferative and secretory proteome of fertile and infertile women

To verify differential expression of various proteins in our human endometrial fluid proteome, we compared our dataset to previous omic-based studies (**Supplementary Tables S1-S3, S6, S10-S11**), that aimed to identify predictors of embryo implantation in IVF cycle [11,12] and/or are a part of the transcriptomic signature of human endometrial receptivity (ERA, endometrial receptivity array) [43] as well as a meta-signature of endometrial receptivity [44] **(Fig. 6-7)**. We further compared our findings with genes involved in endometrium preparation during the WoI for embryonic implantation [45,46] **(Fig. 6-7)**. We verified that 16/186 proteins that are known players of implantation [45,46] and 6/53 proteins predictors of WoI [44], were exclusively identified in the S-phase compared to P-phase (**Fig. 6ab**). Moreover, 4/10 UF proteins associated with implantative success in IVF were also exclusively identified in the S-phase compared to P-phase (**Fig. 6c**). Importantly, transcripts of 15/143 proteins exclusively identified in S-

phase UL are used in the human endometrial receptivity array (ERA) [43] to predict WoI or receptive endometrium ~~(~~**Fig. 6d)**.

For proteins identified in S-phase UL associated with fertility (in comparison to infertile), we verified their expression associated with embryo implantation and endometrial receptivity (**Fig. 7**, **Supplementary Table S12**), identifying 10/186 proteins that are known players of implantation [45,46] and 2/53 proteins predictors of WoI [44] (**Fig. 7ab**). We further report 10 proteins in the UL infertile S-phase proteome associated with implantation failure in IVF cycles [11,12] **(Fig. 7c)**. Moreover, 5/143 proteins exclusively identified in S-phase UL (fertile) have been shown to predict WoI [43] (**Fig. 7d**), while 5/95 proteins in UL infertile S-phase proteome associated with low receptivity (low gene or mRNA expression) in the endometrium during WoI [43] **(Fig. 7d).**

As further validation, we have performed using independent patient cohort and label-free MS-based quantitation **(Supplementary Table S13)**, and identified 57/245 fertile secretory UL proteome as fertility-associated proteins and 106/264 infertile secretory UL proteome as infertility-associated proteins **(Supplementary Table S12)**.

Thus, our findings indicate that sEVs carry proteins known to regulate implantation and predict the WoI, thus highlighting their potential as a minimally invasive biomarker. This study provides a comprehensive insight into proteome reprogramming of sEVs and the soluble secretome in uterine fluid and drives our understanding of infertility and implantation.

Discussion

Dynamic regulation of the proteins in uterine fluid and its sEV components during the menstrual cycle, provides the microenvironment for embryo implantation and establishment of successful pregnancy, yet remains poorly understood. This study presented a comprehensive analysis of this sEV protein landscape using a MS-based proteomic approach to quantify protein expression during distinct phases of the natural menstrual cycle and their dysregulation during infertility. Functionally, both antioxidant and invasive properties were transmitted to trophectoderm cells following sEV uptake. Additionally, the proteins contained within sEVs, were compared with those in the soluble component of uterine fluid. This breadth of new information, combined with published data, enabled development of proliferative and secretory phase UL proteomes in both fertile and infertile women.

Role of uterine fluid sEVs in antioxidant activity

A major finding in our study was the enrichment of antioxidant activity in uterine sEVs in fertile women, which was impeded during infertility. Although this is in line with several studies suggesting that UL contains a variety of antioxidants in the S-phase [9,10,47] which protect pre-implantation embryos by reducing oxidative damage [48,49], to our knowledge, this is the first report of endometrial sEVs transferring antioxidant activity to trophectoderm cells. It is becoming evident that antioxidants protect embryos from ROS-mediated damages, implantation failure and pregnancy loss [31,32]. Recently, Gardner and colleagues demonstrated that exogenous supplementation of antioxidants (acetyl-L-carnitine, N-acetyl-L-cysteine and α-lipoic acid) in IVF media significantly improved development and viability of mouse preimplantation embryos [48,49]. In a prospective clinical trial, these antioxidants in IVF culture media improved human embryo development and transfer outcomes (Trial registration number: NCT02999958). In a developing blastocyst, antioxidants are particularly useful in the trophectoderm as ~50% of glucose is utilized via oxidative phosphorylation to generate ATPs needed to fuel energy consuming Na+/K+ ATPase for blastocoel expansion [50]. Because oxidative phosphorylation results in generation of ROS, embryo- and endometrium-derived antioxidants, for examples those delivered by EVs, potentially ensure embryo protection from oxidative stress-induced damage.

Role of uterine fluid sEVs in trophectoderm invasion during embryo implantation

Our data also indicate that reprogramming of sEV composition during the S-phase potentially facilitates embryo implantation by supporting trophectoderm cell invasion. A crucial step during embryo implantation is its invasion into the endometrium [37] during which trophectoderm cells from the blastocyst invade between endometrial epithelial cells, and through the underlying basement membrane. Then as differentiated trophoblast, they progress through the endometrial stroma with the purpose of reaching maternal blood vessels [51,52]. How acquisition of invasive phenotype is spatially and temporally regulated is not known; from the data presented here, it is likely that sEVs locally released by endometrial epithelium and taken up by the trophectoderm, to initiate invasion. Indeed, a recent study shows that EVs can regulate persistent directional migration of cancer cells, most likely by stabilizing leading edge protrusions [53]. Since there are many molecular commonalities between cancer invasion and metastasis and trophectoderm/trophoblast invasion at implantation [54], it is likely that similar EV cargo in UL-sEV, could be functionally delivered to trophectoderm cells to trigger their initial invasion. Interestingly, we have shown that cancer cell-derived EVs can promote invasion of stromal fibroblasts through Matrigels [55]. Whether these signals are maintained during trophoblast differentiation or whether new signals are provided from the new microenvironment within the decidualizing stroma, should be investigated.

Uterine soluble secretome is enriched in chaperones and glycolytic proteins

Interestingly, UL-T proteome analysis provided insight into pathways that were not enriched in the UL-sEV proteome. For example, S-phase UL-T was enriched in chaperones such as HSP60/70 shown to regulate mouse pre-implantation embryo development [39,40], and chaperonin-containing TCP1 complex components involved in telomerase trafficking and telomere elongation in embryonic stem cells [56]. S-phase UL-T proteins involved in glycolysis are also enriched but could merely reflect changes during the S-phase, whereby progesterone-driven increased glycolysis fuels endometrial receptivity [57,58]. Alternatively, it may assist in meeting the metabolic needs of the human blastocyst within the uterine

cavity: this undergoes aerobic glycolysis associated with replication, maintenance of pluripotency, and in anticipation of a rapid increase in biomass during early stages of implantation [42].

UL proteome provides unique insight into cycle phase and endometrial receptivity: implications for clinical application

As anticipated, the UL proteome reflected phase-specific endometrium phenotype, highlighting its unmet potential to inform on endometrial status. Monitoring uterine fluid expression of receptivity-associated proteins could thus present a tissue biopsy-surrogate to not only define WoI but also predict implantation success [11-13,59,60]. Because the UL proteome between fertile and infertile women also differed for known players of embryo implantation and predictors of WoI or implantation success cycle, it may assist in characterization of endometrium-related alterations linked to infertility and guide UL restoration towards an implantation signature. Interestingly, several of these proteins were detected specifically in sEVs, including predictors of embryo implantation (PRDX2, IDHC), endometrial receptivity (S100A4, FGB, SERPING1, CLU, ANXA2) and implantation success (CAT, YWHAE, PPIA), which can be readily isolated for diagnostic purposes, suggesting the potential that inclusion of UL-sEVs or appropriately engineered nanoparticles at the time of embryo transfer, could improve the potential for implantation and establishment of pregnancy.

Limitations of this study mainly concern the use of human endometrial epithelial model to demonstrate sEVs can perform antioxidant and invasive activity on human trophectoderm cells. Due to the low sEV amount isolated from UL, we did not study the function of UL-derived sEVs, but instead performed cell-based assays to demonstrate function of endometrial-derived sEVs. To investigate endometrial-derived sEV function on human trophectoderm, we employed human trophectoderm cells, grown as spheroids (blastocyst mimic) due to strict ethical regulation in use of human embryos. Understanding the underlying mechanisms of uterine fluid and endometrial cell-derived functional assays on human trophectoderm was not investigated here, presenting an outstanding question in the field. Importantly, we provide in-depth MS-based validation of uterine fluid proteome using a separate, independent

patient cohort, further highlighting key proteins identified in uterine fluid from this study previously implicated in embryo implantation, receptivity, and fertility.

In summary, findings from our data provide new insight into the functions of sEVs in uterine fluid and the molecular basis of infertility. Indeed, the molecular leads identified define the protein and EV content of the physiological pre-implantation endometrial environment, in which final preparation for implantation occurs, how this differs between the proliferative and the receptive secretory phase and between fertile and infertile women. Application of this knowledge may enhance the chance of successful implantation and establishment of pregnancy. Alternatively, it could be applied to the development of a new class of a non-steroidal once-a month contraceptive.

Methods

The materials and methods used in this study are summarized here; more detailed information is available in **Supplementary Information**, **Methods**.

Uterine lavage sample collection

Clinical samples were collected with informed written consent in accordance with the guidelines of the National Health and Medical Research Council (Australia) using protocols reviewed and approved by the Human Research Ethics Committees of Monash Surgical Private Hospital (approval #06066) and Southern Health (approval #03066B). Patient cohorts included fertile women with proven parity undergoing gynecologic procedures e.g. tubal ligation, Mirena® insertion, and from idiopathic primary infertile women undergoing dilatation and curettage **(Table 1, Supplementary Fig. S1)**. Women with diagnoses of male factor infertility, endometriosis, tubal or ovarian abnormalities (e.g., blocked tubes, amenorrhea and polycystic ovarian syndrome) and those using steroidal contraceptives in the prior six months were excluded. Uterine lavage was performed with 5 mL saline (at 37 ^{0}C) infused gently into the uterine cavity through a soft infant feeding tube and recovery by gentle retraction of the syringe [9]. Collected lavage was mixed with 5 µL of protease inhibitor cocktail (Merck KGaA, Darmstadt, Germany) and any mucus removed. Any samples that contained visible blood were discarded. Following centrifugation at 1000 rpm for 10 min the lavage was aspirated and stored as de-identified aliquots at −80 °C prior to analysis. Cycle phase dating on tissue subsequently harvested, was performed by accredited independent pathologists based on Noyes' criteria [61].

Isolation of small EVs

We fractionated uterine lavage into small EVs (UL-sEVs) and soluble secretome (UL-SS) components using differential centrifugation, as previously described [29]. Briefly, uterine lavage was sequentially centrifuged at 500 x *g*, 2,000 x *g* and 10,000 x *g* to remove cellular debris and large EVs (also referred to as microparticles or shed microvesicles) [18], respectively. The supernatant was ultracentrifuged at 100,000 x *g* to obtain UL-sEVs. The UL-sEVs were washed once using 1 mL PBS, re-centrifuged at 100,000 x *g* (1 h) at 4°C and resuspended in PBS. The supernatant represents the UL-SS. Samples were

subjected to total protein quantification using microBCA Protein Assay (Thermo Fisher Scientific). Samples were stored at -80 °C until further use.

Cryo-electron microscopy

Cryo-electron microscopy (cryo-EM) imaging of UL-sEV preparations was performed as described [26]. Briefly, UL-sEVs (~1 μg) were transferred to glow-discharged C-flat holey carbon grids (ProSciTech Pty Ltd). Excess liquid was removed by blotting, and the grids were plunge-frozen in liquid ethane. Grids were mounted in a Gatan cryoholder (Gatan, Inc.) in liquid nitrogen. Images were acquired at 300 kV using a Tecnai G2 F30 (FEI) in low-dose mode.

Proteomic liquid chromatography–tandem mass spectrometry

Protein samples were digested with trypsin and peptide mixture was subjected to tandem mass tag (TMT) multiplexing using TMTsixplex™ Isobaric Label Reagent. Labelled peptides were analyzed on a nanoflow UPLC instrument (Ultimate 3000 RSLCnano, ThermoFisher Scientific) coupled to an Q-Exactive HF Orbitrap mass spectrometer (ThermoFisher Scientific) as described [62]. Label-free MS-based validation study was performed on a separate cohort using single-pot, solid-phase-enhanced sample separation (SP3) and independently analyzed on an Q-Exactive HF-X Orbitrap mass spectrometer (**Supplementary Table S10**). Raw mass spectrometry data is available in ProteomeXchange (#PXD020975).

Bioinformatics

Peptide identification and quantification were performed using MaxQuant (v1.6.6.0) with its built-in search engine Andromeda [63] as described [64]. Perseus [65] was used to quantify proteins whose expression was identified in at least 70% in at least one group; normalized intensities were log2 transformed, with statistical analyses performed using Student's T-test or ANOVA ($P < 0.05$ considered significant). Gene Ontologies (biological processes) were obtained using gProfiler. EnrichmentMap analysis was performed using Cytoscape.

Trophectoderm and endometrial cell culture

Human trophectoderm stem cells L2-TSC and T3-TSC were cultured as described [17]. TSC spheroids were generated using round bottomed ultra-low attachment 96-well plates (Costar). Ishikawa endometrial epithelial cells were maintained in DMEM/F12 supplemented with 1% P/S, and 5% v/v FBS [66].

Estrogen and progesterone priming of endometrial epithelial cells

Hormonal priming of Ishikawa cells was performed as previously described [26]. The conditioned media were subjected to sEV isolation protocol [29], and further purified using OptiPrep™-density gradient-based separation as described [29].

Cellular reactive oxygen species detection assay

ROS detection assay (Abcam) performed according to manufacturer's protocol, where T3-TSC cells were treated with E- or EP-sEVs (50 μg/mL) for 3 h at 37 °C. Control cells were treated with PBS vehicle or L-ascorbic acid (AA) (Wako, 10 μM). Cells were then incubated with DCFDA for 1 h, followed by ROS induction using 50 μM TBHP, and fluorescence measured (excitation/emission 485 nm/535 nm) after 10 min.

Matrigel™ invasion assay

T3-TSC spheroids treated with 50 μg/mL E- or EP-sEVs or PBS vehicle control were assessed for their capacity to invade Matrigel™ over 48 h. Spheroids were imaged using Olympus FSX100.

Uptake of UL-sEVs by trophectoderm cells

Labelling of UL-sEVs was performed at previously described [29]. Pooled UL-sEVs were labelled with 5 mM DiI lipophilic dye (Invitrogen) in PBS for 15 min at 37 °C. Labelled UL-sEVs were ultracentrifuged at 100,000 x *g* for 1 h and washed with 1 mL PBS. The resulting pellet was resuspended

in PBS and overlaid onto L2-TSC cells cultured on a glass coverslip. After 2 h incubation at 37 °C, cells were washed twice with serum free media and nucleus stained with Hoechst (10 mg/mL). Cells were then subjected to live cell imaging using Nikon A1R. Uptake experiments were repeated twice.

Statistical analysis

Data were analyzed using GraphPad Prism 8.0.1 and Microsoft Excel. One-way ANOVA (multiple comparisons) was performed and statistical significance defined at $P < 0.05$.

Acknowledgements: The authors acknowledge L2-/T3-TSC cells were a generous gift from Prof. Susan Fisher (University of California, San Francisco), and the Ishikawa cells were a gift from Prof. Masato Nishida to Prof Guiying Nie and used with approval. The authors thank Judi Hocking for collection of the uterine lavage samples and Drs Tracey Edgell and Jemma Evans for their cataloguing and storage of these. We thank Bio21 Molecular Science and Biotechnology Institute for assisting cryo-electron microscopy (University of Melbourne), Comprehensive Proteomics Platform at La Trobe Institute for Molecular Science (LIMS) (La Trobe University), and Monash Microimaging (Monash University).

Author Contributions

AR, LS, DG designed research; AR, QP, MF, HF, DG performed research; SG, BV, LS contributed human material/reagents/analytic tools; AR, QP, MF, DG analyzed data; AR, DG wrote manuscript; AR, QP, MF, LS, DG reviewed manuscript for submission.

Additional Information

Conflict of Interests: The authors declare no competing or financial interests.

Data availability

All data is included in this published article (and its Supplementary Information files). Raw mass spectrometry data is available in ProteomeXchange (#PXD020975).

Funding: This work was funded in part by NHMRC project grant (#1139489 to LS and DG), Helen Amelia Hains Fellowship (to DG), and by the Victorian State Government Operational Infrastructure funding to the Hudson Institute and Baker Institute.

ORCID

Alin Rai 0000-0001-7994-5151; Qi Hui Poh 0000-0003-2620-2834; Monique Fatmous 0000-0003-4270-6282; Lois A Salamonsen - 0000-0003-0558-7325; David W Greening - 0000-0001-7516-485X

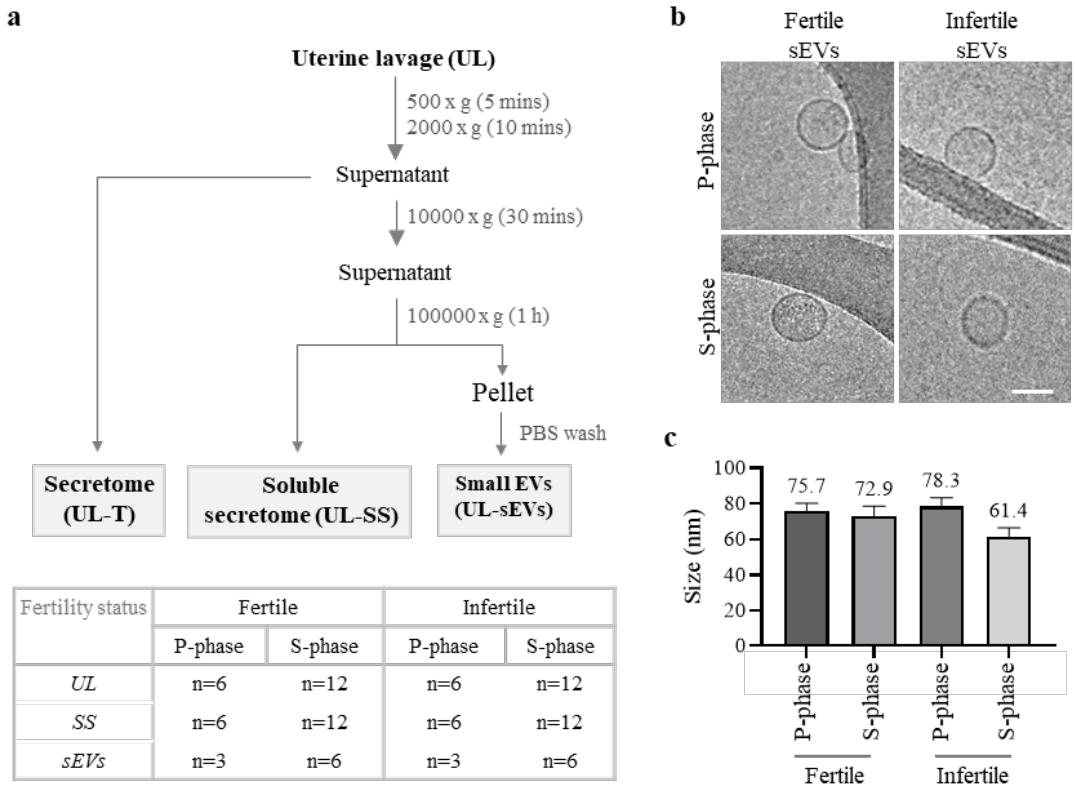

Fertility status	Fertile		Infertile	
	P-phase	S-phase	P-phase	S-phase
UL	n=6	n=12	n=6	n=12
SS	n=6	n=12	n=6	n=12
sEVs	n=3	n=6	n=3	n=6

Fig. 1. Isolation and characterization of small extracellular vesicles (sEV) and soluble secretome (SS) from uterine lavage (UL). **a**, Work flow for isolation of sEVs and SS components from UL using differential centrifugation strategy. The table indicates the number of samples subjected to quantitative mass spectrometry-based proteome profiling in both proliferative phase (P-phase) and secretory phase (S-phase). **b**, Cryo-electron microscopic analysis of UL-sEVs. Scale bar 100 nm, 10 frames per view. **c**, Bar plot representing size distribution (mean ± S.E.M.) of UL-sEVs; number of sEVs measured for their size (diameter) for fertile P-phase (76 nm), fertile S-phase (73 nm), infertile P-phase (78 nm) and infertile S-phase (61 nm), respectively.

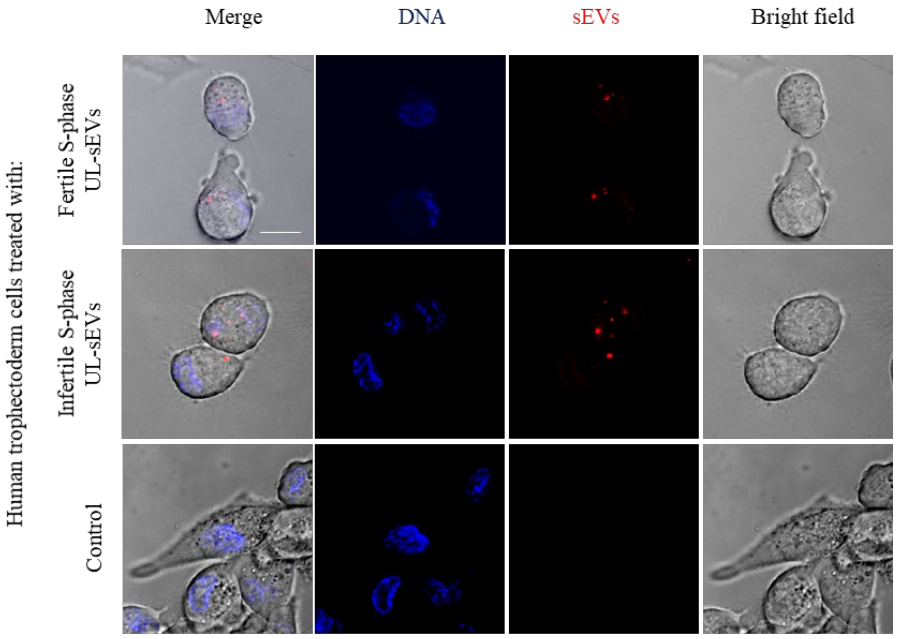

Fig. 2. Uterine fluid-derived UL-sEVs are taken up by human trophectoderm cells. Live fluorescence and brightfield microscopic analysis of human trophectoderm cells (L2-TSCs) incubated with S-phase UL-sEVs (2 h) derived from fertile and infertile women. The UL-sEVs were stained with lipophilic tracer DiI (red). Nuclei were stained with Hoechst (blue). Scale bar: 5 µm.

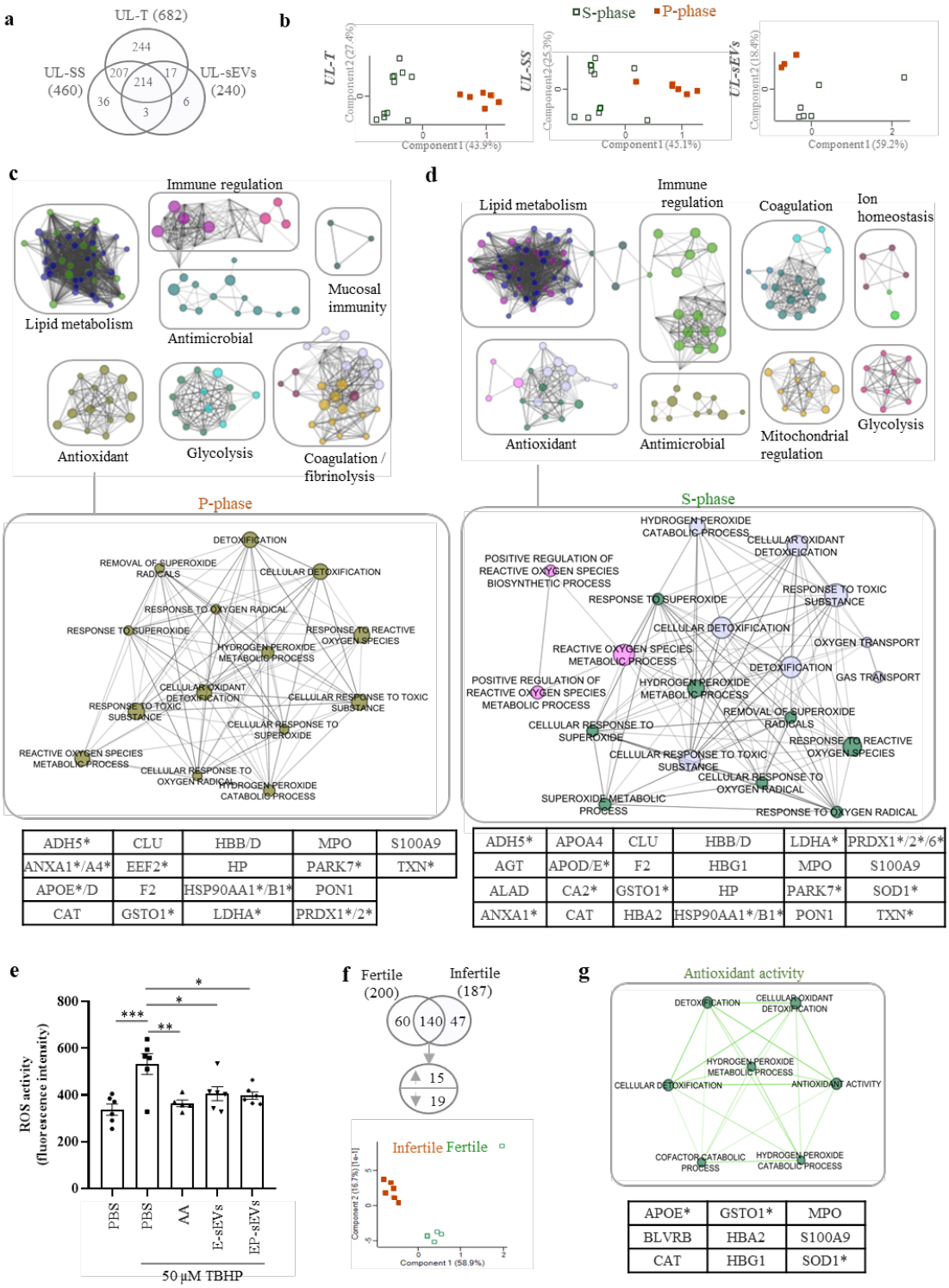

Fig. 3. Endometrial sEVs regulate antioxidant activity in trophectoderm cells. a, Venn diagram of proteins identified in human UL-T, UL-SS and UL-sEVs. **b**, Principal component analysis of proteins (with their respective intensity) identified in UL-T, UL-SS and UL-sEVs during P-phase and S-phase in fertile women. **c**, Upper panel, EnrichmentMap of pathways enriched in P-phase UL-sEVs from fertile women. Lower panel: Antioxidant cluster is highlighted with proteins involved listed beneath it (*proteins present in human endometrial epithelial cell-derived E-sEVs, estrogen treated [26]). **d**, Upper

panel, EnrichmentMap of pathways enriched in S-phase; lower panel: Antioxidant cluster is highlighted with proteins involved listed beneath it (*proteins present in human endometrial epithelial cell-derived EP-sEVs, estrogen-progesterone treated [26]). **e**. Cellular ROS detection assay. Trophectoderm cells were stimulated with E- or EP-sEVs (50 μg/mL, 3 h), then labelled with DCFDA (25 μM, 1 h) and incubated with TBHP (ROS inducer). Cells were then analyzed using fluorescent plate reader with fluorescence intensity directly correlating to ROS activity. Control cells were treated with PBS vehicle or L-ascorbic acid (AA, 10 μM). Bar plot of mean ± S.E.M (N=6)., *p<0.05, **p<0.005, ***p<0.0005. **f**, Venn diagram of proteins identified in fertile and infertile UL-sEVs with proteins significantly up and downregulated (p<0.05, fold change >1.5). Lower panel: PCA of proteins (with their respective intensity) identified in fertile and infertile sEVs. **g**, Antioxidant cluster downregulated in infertile *versus* fertile UL-sEVs with the proteins involved listed beneath (*proteins present in human endometrial epithelial cell-derived EP-sEVs [26]).

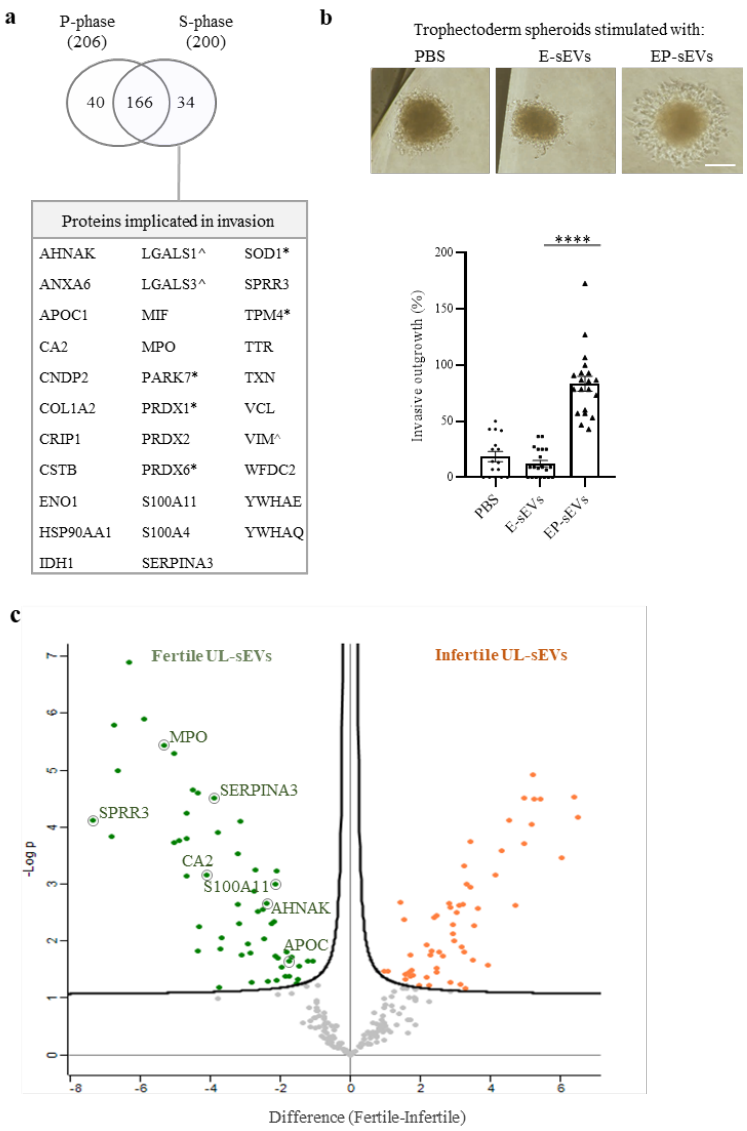

Fig. 4. UL-sEVs confer trophectoderm cells with invasive phenotype. a, Venn diagram of proteins identified in P- and S-phase UL-sEVs from fertile women. Invasion-related proteins found in higher abundance (uniquely identified or fold change >1.5, $p<0.05$) in S-phase UL-sEVs are listed beneath (^proteins previously implicated in trophectoderm cell invasion; *proteins upregulated in human endometrial epithelial cell-derived EP- *versus* E-sEVs [26]. **b**, Trophectoderm spheroid invasion assay. Bright-field microscopy images of trophectoderm spheroids, stimulated with E- or EP-sEVs, invading into Matrigel™ matrix. Scale bar, 100 µm. Lower panel: Bar plot representing invasive outgrowth (mean ± S.E.M.) of trophectoderm spheroids (****$p<0.00005$). **c**, Volcano plot of fold change of proteins in fertile *versus* infertile UL-sEVs. Invasion-related proteins found in higher abundance in S-phase *versus* P-phase sEVs from fertile women are named.

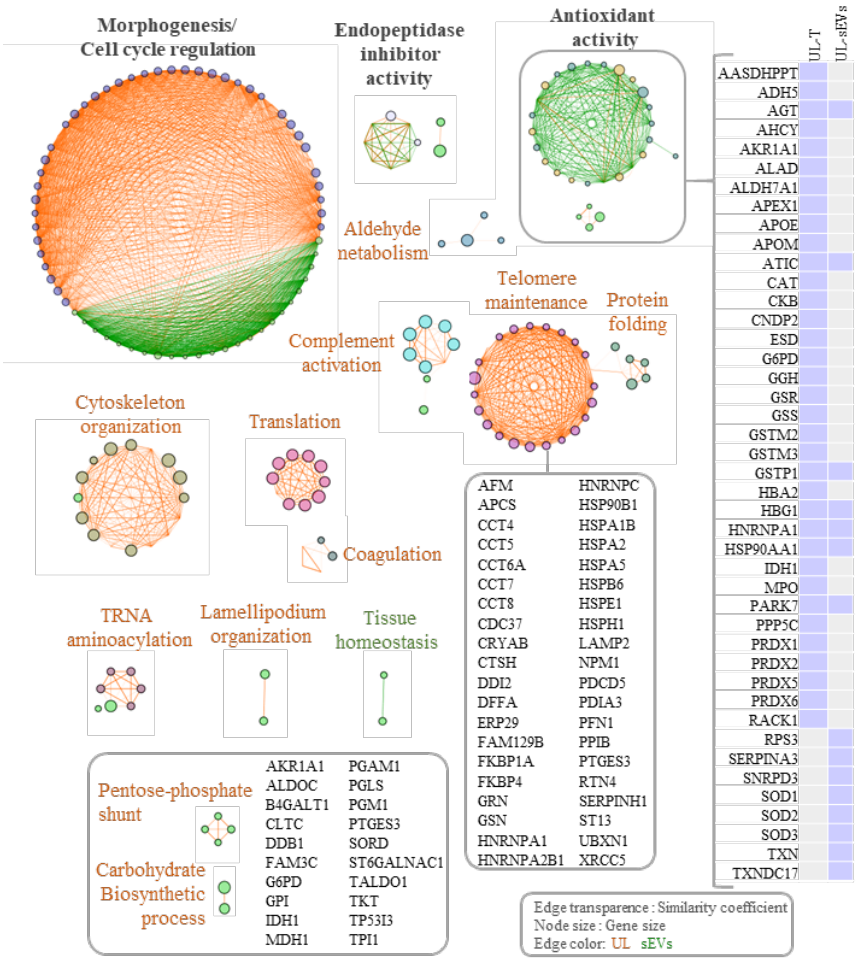

Fig. 5. Phase-specific reprogramming of UL-T and UL-sEVs highlight different biological processes in fertile women. EnrichmentMap of biological pathways enriched in UL-T (orange edge) or UL-sEVs (green edge) in S-phase *versus* P-phase in fertile women. The node size corresponds to the number of proteins involved in that pathway. Proteins implicated in antioxidant activity pathway are listed as a heat map, with blue color indicating enrichment in UL-T or UL-sEVs during the S-phase. Proteins implicated in specified pathways are also listed.

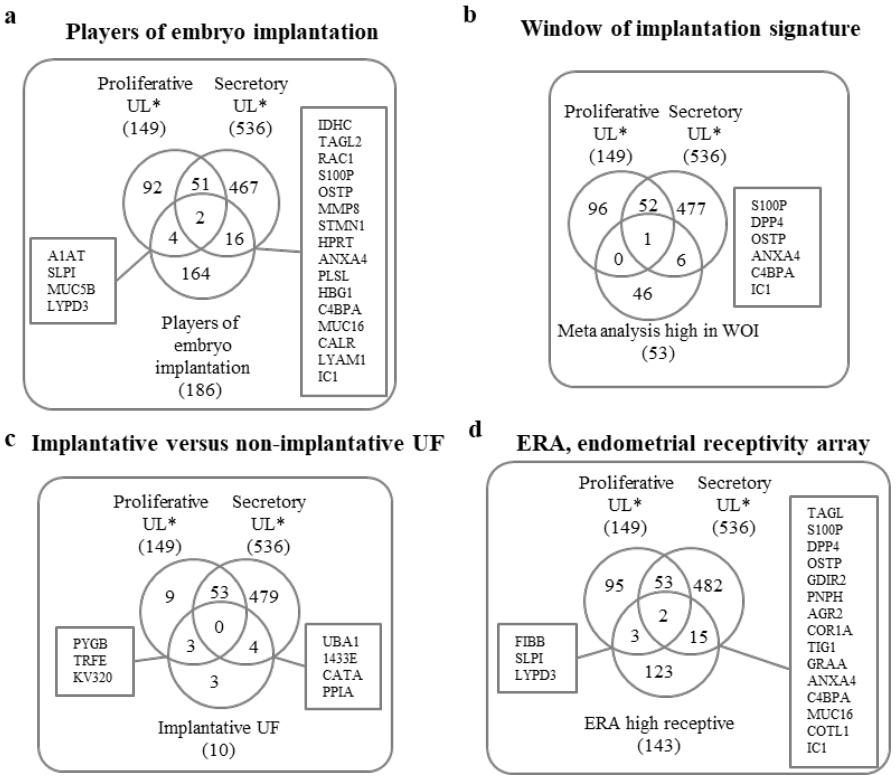

Fig. 6. Validation of phase-specific proteins in UL associated with embryo implantation and endometrial receptivity. a, Venn diagram of UL proliferative and secretory phase proteome with known players of implantation [45,46]. **b**, Venn diagram of UL proliferative and secretory phase proteome with window of implantation [44]. **c,** Venn diagram of UL proliferative and secretory phase proteome with uterine fluid predicting implantation success in IVF cycle [11,12]. **d**, Venn diagram of UL proliferative and secretory phase proteome with endometrial receptivity associated proteins derived from the endometrial receptivity array (ERA) [43].

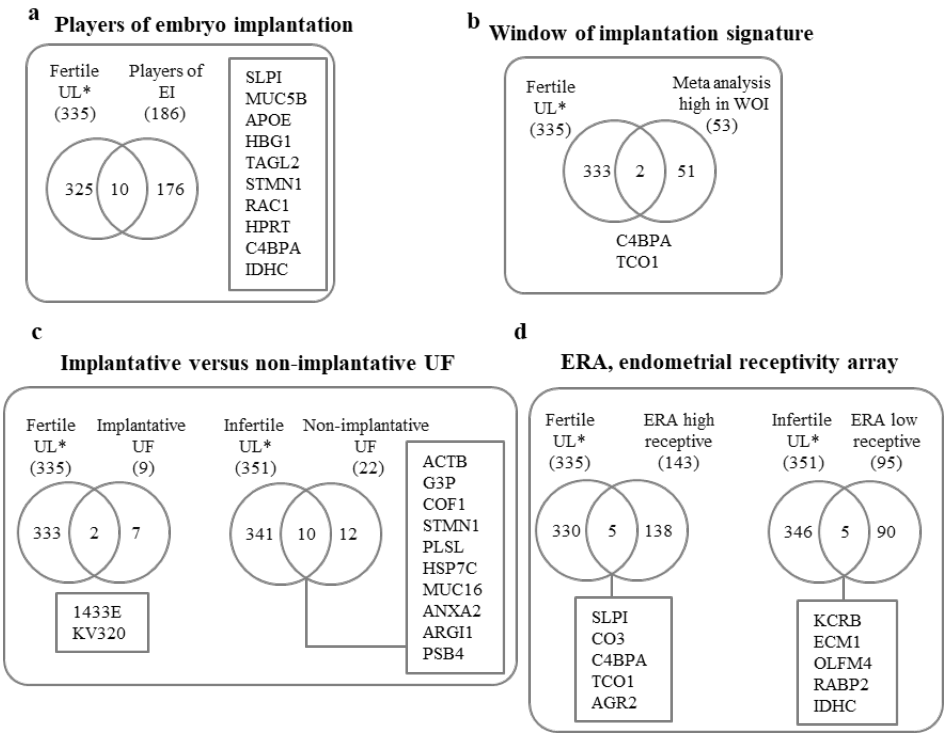

Fig. 7. Validation of implantation and endometrial receptivity associated proteins in fertility associated proteins in UL. a, Venn diagram of fertile UL proteome and known players of implantation [45,46]. **b**, Venn diagram of fertile UL proteome and window of implantation signature [44]. **c**, Venn diagram of fertile UL proteome and UL signature predicting implantation success in IVF cycle [11,12]. **d**, Venn diagram of fertile UL proteome and endometrial receptivity associated proteins in the ERA [43].

Table 1 – Patient cohort

	Sample number	Age	Fertility Status	Pathology cycle phase	UL-T (µg/µL) ^	UL-SS (µg/µL) ^	UL-sEVs (µg/µL) ^
Fertile proliferative	1	40	F	P	1.45	1.24	0.03
	2	34	F	P	2.36	1.99	0.15*
	3	46	F	P	0.57	0.41	0.15*
	4	44	F	P	0.69	0.46	0.22*
	5	30	F	P	0.70	0.61	0.03
	6	32	F	P	0.41	0.40	0.02
Fertile secretory	1	32	F	E-M	1.69	1.46	0.02
	2	30	F	E	3.20	3.11	0.05*
	3	38	F	E	1.46	1.23	0.01
	4	35	F	E	1.34	1.19	0.11*
	5	31	F	E-M	0.80	0.76	0.06*
	6	33	F	M	5.35	5.19	0.31
	7	36	F	E	0.74	0.69	0.03*
	8	35	F	M	0.38	0.29	0.01
	9	38	F	M	0.93	0.90	0.02
	10	36	F	M-L	0.63	0.61	0.02
	11	36	F	M	1.52	1.49	0.06*
	12	42	F	E	0.66	0.62	0.02*
Infertile proliferative	1	30	I	P	1.54	1.43	0.10*
	2	28	I	P	1.10	1.01	0.07*
	3	36	I	P	1.28	1.23	0.10*
	4	30	I	M-L P	0.73	0.65	0.06
	5	29	I	M P	0.55	0.52	0.16
	6	33	I	P	0.61	0.56	0.02
Infertile secretory	1	29	I	M-L	1.10	1.16	0.03*
	2	36	I	M-L	0.38	0.30	0.00
	3	37	I	M-L	1.17	1.06	0.01*
	4	38	I	M	0.50	0.49	0.00
	5	39	I	M	0.45	0.42	0.00
	6	33	I	M	0.41	0.40	0.01
	7	35	I	M	0.86	0.79	0.01
	8	28	I	M	2.11	1.95	0.01*
	9	37	I	M-L	1.55	1.41	0.05*
	10	35	I	M	0.85	0.82	0.01*
	11	39	I	M	0.96	0.86	0.02*
	12	35	I	M	0.48	0.40	0.03

F= fertile, I= infertile, P=proliferative phase; E, M, L – early, mid and late secretory phases respectively; *sEV samples subjected to mass spectrometry analysis; ^protein concentration

Table 2 – Invasion-related proteins enriched in S-phase *versus* P-phase UL-sEVs in fertile women

Gene name	Protein description	Function	Ref (PMIDs)
AHNAK	Neuroblast differentiation-associated protein AHNAK	Regulates invasion through epithelial-mesenchymal transition (EMT) through regulation of AKT/MAPK and Wnt/β-catenin signalling pathways	30258109, 24253341
ANXA6	Annexin A6	Regulates invasion by modulating cell migration and adhesion through cytoskeletal rearrangement, and membrane-bound components	21185831, 28060548
APOC1	Apolipoprotein C-I	Influences cell proliferation and motility via the MAPK pathways to regulate invasion	31213910
CA2	Carbonic anhydrase 2	Invasion-associated factor that plays a role in making surrounding environment acidic to promote cell invasiveness.	28004470
CNDP2	Cytosolic non-specific dipeptidase	Promotes invasion by increasing PI3K-AKT phosphorylation (previously shown to enhance cell metastasis in ovarian cancer).	31537175
COL1A2	Collagen alpha-2	Major component of ECM and therefore its ability to remodel ECM influences invasion.	28482162, 32566007
CRIP1	Cysteine-rich protein 1	Mediates cell migration and invasion through EMT and Wnt/β-catenin signaling pathway.	29179181, 29959029, 31312368, 29059670
CSTB	Cystatin-B	Promote invadopodia formation which utilize MMPs to degrade ECM and promote invasion.	32029550
ENO1	Alpha-enolase	Important interaction with alpha v/beta 3 integrin and urokinase plasminogen activator receptor (uPAR) to promote invasion and migration.	28086938
HSP90AA1	Heat shock protein HSP 90-alpha	Act as an extracellular chaperone to activate MMP2 and promote ECM degradation for invasion.	15146192
IDH1	Isocitrate dehydrogenase [NADP] cytoplasmic	Contributes to invasion by promoting proliferation and migration through EMT and Wnt/β-catenin signaling.	26860959, 31983120, 29115585
LGALS1	Galectin-1	Influence trophectoderm cell adhesion, migration and invasion through complex lectin type interaction with β1 integrin and increase in MMP2/9, ZEB-1, and N-cadherin while decreasing E-cadherin expression.	22174828, 28826368, 28992109, 29122660
LGALS3	Galectin-3	Involved in trophoblast invasion. Present in high levels in invasive extravillous trophoblast, promotes migration through pFAK, MAPK/ERK-1/2, pERK1/2 and pAkt, and invasion through β-catenin to increase MMP activity during invasion.	30765738, 22174828, 24809457
MIF	Macrophage migration inhibitory factor	Promotes invasion by cytoskeletal reorganization and pseudo foot formation through EMT induction.	17142775, 30667094
MPO	Myeloperoxidase	Present in fetal-maternal interface, reacts with H2O2 to produce HOCl which modifies proteins at the site of trophoblast invasion into maternal tissue. It also stimulates the maternal immune system.	28260049, 11304574
PARK7	Protein/nucleic acid deglycase DJ-1	Promotes invasion through the SRC/ERK/uPA cascade.	27186306, 22223849
PRDX1	Peroxiredoxin-1	Associates with formation of membrane protrusions through modulation of p38 MAPK activity to promote invasion.	25426613
PRDX2	Peroxiredoxin-2	Promotes migration and invasion through MMP9 expression.	32337219
PRDX6	Peroxiredoxin-6	Exhibits phospholipase (PLA2) activity to activate Akt via phosphoinositide 3-kinase (PI3K) and p38 kinase to promote cell invasion.	20354123
S100A11	Protein S100-A11	S100A11 promotes EMT required for invasion by regulating Snail (upregulated) and E-cadherin proteins (downregulated).	28513300, 25780452
S100A4	Protein S100-A4	Promotes migration and invasion by inducing TGF-β-mediated EMT and upregulating NDUFS2.	23308057, 30410586, 30885944
SERPINA3	Alpha-1-antichymotrypsin	Expression correlates with MMP2/9 expression to enhance cell invasion and migration.	29855767
SOD1	Superoxide dismutase [Cu-Zn]	Promotes invasion and migration by influencing cell cycle and apoptosis.	32391354
SPRR3	Small proline-rich protein 3	Promotes both proliferation and invasion through AKT activation and p53 reduction.	24396461
TPM4	Tropomyosin alpha-4 chain	Promotes cell motility by altering actin cytoskeleton through F-actin modulation.	31239699
TTR	Transthyretin	Regulate trophoblast invasion and migration by increasing MMP2/9 for ECM degradation.	28454241
TXN	Thioredoxin	Overexpression of TXN increases MMP-9 expression, promoting ECM degradation and cell invasion.	28483515 26760912
VCL	Vinculin	Modulates cell adhesion and motility through mechanical link of contractile actomyosin cytoskeleton to the ECM through integrin receptors.	25183785, 20181946, 28783415
VIM	Vimentin	Involved in blastocyst invasion by promoting cell migration through integration of mechanical input from the environment and modulating the dynamics of microtubules and actomyosin network.	17512929, 30505430
WFDC2	WAP four-disulfide core domain protein 2	Promotes EMT by activating AKT signalling pathway and inducing MMP2 expression.	31118763
YWHAE	14-3-3 protein epsilon	Promotes proliferation, migration and invasion through ERK/MAPK pathway, Rac1/Tiam1 signaling, possibly through expression of Snail and Twist, and also via MMP2/9.	26730736, 31001932, 22899242, 30550728
YWHAQ	14-3-3 protein theta	Promotes invasion by binding phosphorylated RhoGDIα upon EGF stimulation, to release Rho GTPases and promote EGF-induced RhoA, Rac1, and Cdc42 activation.	26083935, 24820414

Table 3 – Invasion-related proteins down-regulated in S-phase UL-sEVs during infertility

Gene name	Protein description	Function	Ref (PMIDs)
A2ML1	Alpha-2-macroglobulin-like protein 1	Found to be important in animals with invasive placenta, but mechanism unknown.	32198464
AHNAK	Neuroblast differentiation-associated protein AHNAK	Regulate proliferation and invasion through epithelial-mesenchymal transition (EMT) by modulation of AKT/MAPK and Wnt/β-catenin signaling pathways.	30258109, 24253341
ANXA1	Annexin A1	Regulates cytoskeletal dynamics, reduction of adhesion molecules and EMT to promote invasion.	27834582
APOC1	Apolipoprotein C-I	Regulates cell migration and invasion possibly via the MAPK pathways.	31213910
APOD	Apolipoprotein D	Interacts with COX-2 to enhance cell invasiveness and motility.	32306242
APOE	Apolipoprotein E	Alters expression of invasion-related proteins including MM7, through cellular cholesterol and AP-1 activity.	28751006
AZGP1	Zinc-alpha-2-glycoprotein	Regulates invasive potential by mediating TGF-β1-ERK2 signaling, and EMT by associating with molecules involved in the focal adhesion pathway, including FLNA.	30820960, 31632499
BPIFB1	BPI fold-containing family B member 1	Regulates cell migration and invasion via EMT through vitronectin and vimentin, and FAK/Src/ERK signaling pathway.	29123267
CA2	Carbonic anhydrase 2	Invasion-associated factor that plays a role in making surrounding environment acidic to promote cell invasiveness.	28004470
CAT	Catalase	Modulate migration and invasion of cells by controlling cathepsin activity.	30655847
CSTA	Cystatin-A	Regulates MET by reducing ERK, p-38 and Akt activity, and prevents EMT induced by TGF-β1 through the ERK/MAPK pathway.	29581829
FABP5	Fatty acid-binding protein 5	FABP5 increased cell invasiveness by increasing the expression of MMP-9.	20040021
MPO	Myeloperoxidase	Present in fetal-maternal interface, reacts with H2O2 to produce HOCl which modifies proteins at the site of trophoblast invasion into maternal tissue. It also stimulates the maternal immune system.	28260049, 11304574
MUC5B	Mucin-5B	Involved in proliferation, migration, and invasion through alteration of β-catenin expression, localization, and activity, hence mediating the Wnt/β-catenin signaling pathway.	28972071
PEBP1	Phosphatidylethanolamine-binding protein 1	Regulates migration and invasion via RAF1/MEK/ERK signaling and modulation of miRNAs.	29436617
PLG	Plasminogen	Invasion - activates MMP9, leading to localized matrix proteolysis as trophoblast invasion commences.	21075828
S100A11	Protein S100-A11	S100A11 promotes EMT required for invasion by regulating Snail (upregulated) and E-cadherin proteins (downregulated)	28513300, 25780452
S100A8	Protein S100-A8	Pro-inflammatory factor, associated with increased MMP2/12 promoting invasion	23456298
S100A9	Protein S100-A9	Pro-inflammatory factor, associated with increased MMP2/12 promoting invasion	23456298
SERPINA3	Alpha-1-antichymotrypsin	Expression correlates with MMP2/9 expression to enhance cell invasion and migration	29855767
SERPINA5	Plasma serine protease inhibitor	Associated with inhibiting tumor invasion (inhibits urinary plasminogen activator (uPA), a mediator of tumor cell invasion, inhibits tumor cell migration by modulating the fibronectin-integrin β1 signaling pathway)	24388360, 17450526
SERPINB3	Serpin B3	Induces epithelial-mesenchymal transition, cell scattering, migration and invasiveness (in vitro)	20527027
SLPI	Antileukoproteinase	Promotes tumor invasion (in conjunction with MMP-2/9) in human uterus myoma	27238568
SPRR3	Small proline-rich protein 3	Promotes proliferation and invasion through AKT activation and p53 reduction	24396461
TFF3	Trefoil factor 3	Promotes invasion in non-malignant cells through alteration of invasion-related genes (no change in proliferation), and stimulates invasion and angiogenesis in vitro.	15680474, 22341453
TKT	Transketolase	Counteracts oxidative stress (redox homeostasis) to drive cancer development (cell invasion, migration, EMT process and tumor microsatellite formation)	26811478, 27698919
TPI1	Triosephosphate isomerase	Crucial enzyme in the carbohydrate metabolism (glycolysis and gluconeogenesis), invasion related in cancer cells	27908734

References

1 Gray, C. A., Burghardt, R. C., Johnson, G. A., Bazer, F. W. & Spencer, T. E. Evidence that absence of endometrial gland secretions in uterine gland knockout ewes compromises conceptus survival and elongation. *Reproduction* **124**, 289-300 (2002).

2 Spencer, T. E. & Gray, C. A. Sheep uterine gland knockout (UGKO) model. *Methods Mol Med* **121**, 85-94, doi:10.1385/1-59259-983-4:083 (2006).

3 van der Weijden, V. A. *et al.* Uterine fluid proteome changes during diapause and resumption of embryo development in roe deer (Capreolus capreolus). *Reproduction* **158**, 13-24, doi:10.1530/REP-19-0022 (2019).

4 Salamonsen, L. A., Evans, J., Nguyen, H. P. & Edgell, T. A. The Microenvironment of Human Implantation: Determinant of Reproductive Success. *American journal of reproductive immunology (New York, N.Y. : 1989)* **75**, 218-225, doi:10.1111/aji.12450 (2016).

5 Zhang, Y., Wang, Q., Wang, H. & Duan, E. Uterine Fluid in Pregnancy: A Biological and Clinical Outlook. *Trends in molecular medicine* **23**, 604-614, doi:10.1016/j.molmed.2017.05.002 (2017).

6 Gray, C. A. *et al.* Endometrial glands are required for preimplantation conceptus elongation and survival. *Biol Reprod* **64**, 1608-1613, doi:10.1095/biolreprod64.6.1608 (2001).

7 Dunlap, K. A. *et al.* Postnatal deletion of Wnt7a inhibits uterine gland morphogenesis and compromises adult fertility in mice. *Biol Reprod* **85**, 386-396, doi:10.1095/biolreprod.111.091769 (2011).

8 Casado-Vela, J. *et al.* Comprehensive proteomic analysis of human endometrial fluid aspirate. *J Proteome Res* **8**, 4622-4632, doi:10.1021/pr9004426 (2009).

9 Hannan, N. J. *et al.* 2D-DiGE analysis of the human endometrial secretome reveals differences between receptive and nonreceptive states in fertile and infertile women. *J Proteome Res* **9**, 6256-6264, doi:10.1021/pr1004828 (2010).

10 Scotchie, J. G., Fritz, M. A., Mocanu, M., Lessey, B. A. & Young, S. L. Proteomic analysis of the luteal endometrial secretome. *Reprod Sci* **16**, 883-893, doi:10.1177/1933719109337165 (2009).

11 Matorras, R. *et al.* Proteomic pattern of implantative human endometrial fluid in in vitro fertilization cycles. *Archives of gynecology and obstetrics* **297**, 1577-1586, doi:10.1007/s00404-018-4753-1 (2018).

12 Azkargorta, M. *et al.* Differential proteomic analysis of endometrial fluid suggests increased inflammation and impaired glucose metabolism in non-implantative IVF cycles and pinpoints PYGB as a putative implantation marker. *Hum Reprod* **33**, 1898-1906, doi:10.1093/humrep/dey274 (2018).

13 Kasvandik, S. *et al.* Uterine Fluid Proteins for Minimally Invasive Assessment of Endometrial Receptivity. *J Clin Endocrinol Metab* **105**, doi:10.1210/clinem/dgz019 (2020).

14 Ng, Y. H. *et al.* Endometrial exosomes/microvesicles in the uterine microenvironment: a new paradigm for embryo-endometrial cross talk at implantation. *PloS one* **8**, e58502, doi:10.1371/journal.pone.0058502 (2013).

15 Campoy, I. *et al.* Exosome-like vesicles in uterine aspirates: a comparison of ultracentrifugation-based isolation protocols. *J Transl Med* **14**, 180, doi:10.1186/s12967-016-0935-4 (2016).

16 Tannetta, D., Dragovic, R., Alyahyaei, Z. & Southcombe, J. Extracellular vesicles and reproduction-promotion of successful pregnancy. *Cell Mol Immunol* **11**, 548-563, doi:10.1038/cmi.2014.42 (2014).

17 Evans, J. *et al.* Human Endometrial Extracellular Vesicles Functionally Prepare Human Trophectoderm Model for Implantation: Understanding Bidirectional Maternal-Embryo Communication. *Proteomics* **19**, e1800423, doi:10.1002/pmic.201800423 (2019).

18 Xu, R. *et al.* Extracellular vesicles in cancer - implications for future improvements in cancer care. *Nat Rev Clin Oncol* **15**, 617-638, doi:10.1038/s41571-018-0036-9 (2018).

19 Park, K. H. *et al.* Ca2+ signaling tools acquired from prostasomes are required for progesterone-induced sperm motility. *Sci Signal* **4**, ra31, doi:10.1126/scisignal.2001595 (2011).
20 Pons-Rejraji, H. *et al.* Prostasomes: inhibitors of capacitation and modulators of cellular signalling in human sperm. *Int J Androl* **34**, 568-580, doi:10.1111/j.1365-2605.2010.01116.x (2011).
21 Siciliano, L., Marciano, V. & Carpino, A. Prostasome-like vesicles stimulate acrosome reaction of pig spermatozoa. *Reprod Biol Endocrinol* **6**, 5, doi:10.1186/1477-7827-6-5 (2008).
22 Murdica, V. *et al.* In vitro cultured human endometrial cells release extracellular vesicles that can be uptaken by spermatozoa. *Sci Rep* **10**, 8856, doi:10.1038/s41598-020-65517-9 (2020).
23 Santonocito, M. *et al.* Molecular characterization of exosomes and their microRNA cargo in human follicular fluid: bioinformatic analysis reveals that exosomal microRNAs control pathways involved in follicular maturation. *Fertil Steril* **102**, 1751-1761 e1751, doi:10.1016/j.fertnstert.2014.08.005 (2014).
24 Miyado, K. *et al.* The fusing ability of sperm is bestowed by CD9-containing vesicles released from eggs in mice. *Proc Natl Acad Sci U S A* **105**, 12921-12926, doi:10.1073/pnas.0710608105 (2008).
25 Bridi, A., Perecin, F. & Silveira, J. C. D. Extracellular Vesicles Mediated Early Embryo-Maternal Interactions. *Int J Mol Sci* **21**, doi:10.3390/ijms21031163 (2020).
26 Greening, D. W., Nguyen, H. P., Elgass, K., Simpson, R. J. & Salamonsen, L. A. Human Endometrial Exosomes Contain Hormone-Specific Cargo Modulating Trophoblast Adhesive Capacity: Insights into Endometrial-Embryo Interactions. *Biol Reprod* **94**, 38, doi:10.1095/biolreprod.115.134890 (2016).
27 Gurung, S., Greening, D. W., Catt, S., Salamonsen, L. & Evans, J. Exosomes and soluble secretome from hormone-treated endometrial epithelial cells direct embryo implantation. *Mol Hum Reprod*, doi:10.1093/molehr/gaaa034 (2020).
28 Greening, D. W., Xu, R., Ji, H., Tauro, B. J. & Simpson, R. J. A protocol for exosome isolation and characterization: evaluation of ultracentrifugation, density-gradient separation, and immunoaffinity capture methods. *Methods in Molecular Biology* **1295**, 179-209 (2015).
29 Rai, A. *et al.* Exosomes Derived from Human Primary and Metastatic Colorectal Cancer Cells Contribute to Functional Heterogeneity of Activated Fibroblasts by Reprogramming Their Proteome. *Proteomics* **19**, e1800148, doi:10.1002/pmic.201800148 (2019).
30 Keerthikumar, S. *et al.* ExoCarta: A Web-Based Compendium of Exosomal Cargo. *J Mol Biol* **428**, 688-692, doi:10.1016/j.jmb.2015.09.019 (2016).
31 Hirota, Y. *et al.* Uterine FK506-binding protein 52 (FKBP52)-peroxiredoxin-6 (PRDX6) signaling protects pregnancy from overt oxidative stress. *Proc Natl Acad Sci U S A* **107**, 15577-15582, doi:10.1073/pnas.1009324107 (2010).
32 Jauniaux, E., Poston, L. & Burton, G. J. Placental-related diseases of pregnancy: Involvement of oxidative stress and implications in human evolution. *Hum Reprod Update* **12**, 747-755, doi:10.1093/humupd/dml016 (2006).
33 Akram, N. A., Shafiq, F. & Ashraf, M. Ascorbic Acid-A Potential Oxidant Scavenger and Its Role in Plant Development and Abiotic Stress Tolerance. *Frontiers in Plant Science* **8**, doi:10.3389/fpls.2017.00613 (2017).
34 Kolundžić, N. *et al.* Galectin-1 Is Part of Human Trophoblast Invasion Machinery - A Functional Study In Vitro. *PloS one* **6**, e28514, doi:10.1371/journal.pone.0028514 (2011).
35 Bojić-Trbojević, Ž. *et al.* Human trophoblast requires galectin-3 for cell migration and invasion. *Scientific Reports* **9**, 2136, doi:10.1038/s41598-018-38374-w (2019).
36 Ivaska, J., Pallari, H. M., Nevo, J. & Eriksson, J. E. Novel functions of vimentin in cell adhesion, migration, and signaling. *Exp Cell Res* **313**, 2050-2062, doi:10.1016/j.yexcr.2007.03.040 (2007).

37 Ochoa-Bernal, M. A. & Fazleabas, A. T. Physiologic Events of Embryo Implantation and Decidualization in Human and Non-Human Primates. *International Journal of Molecular Sciences* **21**, 1973 (2020).
38 Hernandez-Vargas, P., Munoz, M. & Dominguez, F. Identifying biomarkers for predicting successful embryo implantation: applying single to multi-OMICs to improve reproductive outcomes. *Hum Reprod Update* **26**, 264-301, doi:10.1093/humupd/dmz042 (2020).
39 Abdi, Z. *et al.* The effect of HSP60 on fertilization and pre-implantation embryo development in mice: An *in vitro* study. *Acta Endocrinol (Buchar)* **15**, 153-157, doi:10.4183/aeb.2019.153 (2019).
40 Esfandiari, N., Falcone, T., Goldberg, J. M., Agarwal, A. & Sharma, R. K. Heat-shock proteins modulate the incidence of apoptosis and oxidative stress in preimplantation mouse embryos. *Fertil Steril* **87**, 1214-1217, doi:10.1016/j.fertnstert.2006.07.1536 (2007).
41 Kim, J. H. *et al.* Higher maternal vitamin D concentrations are associated with longer leukocyte telomeres in newborns. *Matern Child Nutr* **14**, doi:10.1111/mcn.12475 (2018).
42 Chason, R. J., Csokmay, J., Segars, J. H., DeCherney, A. H. & Armant, D. R. Environmental and epigenetic effects upon preimplantation embryo metabolism and development. *Trends Endocrinol Metab* **22**, 412-420, doi:10.1016/j.tem.2011.05.005 (2011).
43 Diaz-Gimeno, P. *et al.* A genomic diagnostic tool for human endometrial receptivity based on the transcriptomic signature. *Fertil Steril* **95**, 50-60, 60 e51-15, doi:10.1016/j.fertnstert.2010.04.063 (2011).
44 Altmae, S. *et al.* Meta-signature of human endometrial receptivity: a meta-analysis and validation study of transcriptomic biomarkers. *Sci Rep* **7**, 10077, doi:10.1038/s41598-017-10098-3 (2017).
45 Enciso, M. *et al.* Development of a new comprehensive and reliable endometrial receptivity map (ER Map/ER Grade) based on RT-qPCR gene expression analysis. *Hum Reprod* **33**, 220-228, doi:10.1093/humrep/dex370 (2018).
46 Wilcox, A. J., Baird, D. D. & Weinberg, C. R. Time of implantation of the conceptus and loss of pregnancy. *N Engl J Med* **340**, 1796-1799, doi:10.1056/NEJM199906103402304 (1999).
47 Manohar, M. *et al.* Alteration in endometrial proteins during early- and mid-secretory phases of the cycle in women with unexplained infertility. *PloS one* **9**, e111687, doi:10.1371/journal.pone.0111687 (2014).
48 Truong, T. & Gardner, D. K. Antioxidants improve IVF outcome and subsequent embryo development in the mouse. *Hum Reprod* **32**, 2404-2413, doi:10.1093/humrep/dex330 (2017).
49 Truong, T. T., Soh, Y. M. & Gardner, D. K. Antioxidants improve mouse preimplantation embryo development and viability. *Hum Reprod* **31**, 1445-1454, doi:10.1093/humrep/dew098 (2016).
50 Houghton, F. D., Humpherson, P. G., Hawkhead, J. A., Hall, C. J. & Leese, H. J. Na+, K+, ATPase activity in the human and bovine preimplantation embryo. *Dev Biol* **263**, 360-366, doi:10.1016/j.ydbio.2003.07.014 (2003).
51 Carter, A. M., Enders, A. C. & Pijnenborg, R. The role of invasive trophoblast in implantation and placentation of primates. *Philos Trans R Soc Lond B Biol Sci* **370**, 20140070-20140070, doi:10.1098/rstb.2014.0070 (2015).
52 Cha, J., Sun, X. & Dey, S. K. Mechanisms of implantation: strategies for successful pregnancy. *Nature Medicine* **18**, 1754-1767, doi:10.1038/nm.3012 (2012).
53 Sung, B. H., Ketova, T., Hoshino, D., Zijlstra, A. & Weaver, A. M. Directional cell movement through tissues is controlled by exosome secretion. *Nature Communications* **6**, 7164, doi:10.1038/ncomms8164 (2015).
54 Manzo, G. Similarities Between Embryo Development and Cancer Process Suggest New Strategies for Research and Therapy of Tumors: A New Point of View. *Front Cell Dev Biol* **7**, 20-20, doi:10.3389/fcell.2019.00020 (2019).

55 Rai, A., Greening, D. W., Xu, R., Suwakulsiri, W. & Simpson, R. J. Exosomes Derived from the Human Primary Colorectal Cancer Cell Line SW480 Orchestrate Fibroblast-Led Cancer Invasion. *Proteomics* **20**, e2000016, doi:10.1002/pmic.202000016 (2020).

56 Freund, A. *et al.* Proteostatic control of telomerase function through TRiC-mediated folding of TCAB1. *Cell* **159**, 1389-1403, doi:10.1016/j.cell.2014.10.059 (2014).

57 Frolova, A. I. & Moley, K. H. Quantitative analysis of glucose transporter mRNAs in endometrial stromal cells reveals critical role of GLUT1 in uterine receptivity. *Endocrinology* **152**, 2123-2128, doi:10.1210/en.2010-1266 (2011).

58 von Wolff, M., Ursel, S., Hahn, U., Steldinger, R. & Strowitzki, T. Glucose transporter proteins (GLUT) in human endometrium: expression, regulation, and function throughout the menstrual cycle and in early pregnancy. *J Clin Endocrinol Metab* **88**, 3885-3892, doi:10.1210/jc.2002-021890 (2003).

59 Edgell, T. A., Rombauts, L. J. & Salamonsen, L. A. Assessing receptivity in the endometrium: the need for a rapid, non-invasive test. *Reprod Biomed Online* **27**, 486-496, doi:10.1016/j.rbmo.2013.05.014 (2013).

60 Edgell, T. A. *et al.* Assessment of potential biomarkers of pre-receptive and receptive endometrium in uterine fluid and a functional evaluation of the potential role of CSF3 in fertility. *Cytokine* **111**, 222-229, doi:10.1016/j.cyto.2018.08.026 (2018).

61 Noyes, R. W., Hertig, A. T. & Rock, J. Dating the endometrial biopsy. *Am J Obstet Gynecol* **122**, 262-263, doi:10.1016/s0002-9378(16)33500-1 (1975).

62 Greening, D. W. *et al.* Chronic methamphetamine interacts with BDNF Val66Met to remodel psychosis pathways in the mesocorticolimbic proteome. *Mol Psychiatry*, In Press, doi:10.1038/s41380-019-0617-8 (2019).

63 Cox, J. & Mann, M. MaxQuant enables high peptide identification rates, individualized p.p.b.-range mass accuracies and proteome-wide protein quantification. *Nat Biotechnol* **26**, 1367-1372, doi:10.1038/nbt.1511 (2008).

64 Kompa, A. R. *et al.* Sustained subcutaneous delivery of secretome of human cardiac stem cells promotes cardiac repair following myocardial infarction. *Cardiovasc Res*, doi:10.1093/cvr/cvaa088 (2020).

65 Tyanova, S. *et al.* The Perseus computational platform for comprehensive analysis of (prote)omics data. *Nat Methods* **13**, 731-740, doi:10.1038/nmeth.3901 (2016).

66 Evans, J., Walker, K. J., Bilandzic, M., Kinnear, S. & Salamonsen, L. A. A novel “embryo-endometrial” adhesion model can potentially predict “receptive” or “non-receptive” endometrium. *Journal of Assisted Reproduction and Genetics* **37**, 5-16, doi:10.1007/s10815-019-01629-0 (2020).